Thai Journal of Radiological Technology 2006 ; 31(1) : 1-8

A Study of Physical Performance Characteristics of Single and Multislice CT

Manus Mongkolsuk, M.Sc.(Physics)
Napapong Pongnapang, Ph.D.(Medical Physics)

Department of Radiological Technology, Faculty of Medical Technology,
Mahidol University, Bangkok 10700

Abstract

The study was carried out to compare the physical performance characteristics and radiation dose of four unique CT scanners and investigate the effects of slice thickness and pitch. These scanners included a 4th generation conventional CT (PQ2000, Picker), a 3rd generation single slice CT (Asteion, Toshiba), and two multislice CT (LightSpeed Plus, General Electric Medical Systems and Somatom Sensation 64, Siemens). Physical performance characteristics were evaluated in terms of image noise, uniformity, low contrast resolution, high contrast resolution, and slice thickness accuracy, each in comparison to the performance measured on a conventional CT scanner. A Catphan phantom was used to characterize for both axial and helical modes of scanning. The radiation dose measurements were taken from a pencil ionization chamber supported free in air at the center of the CT gantry. Results from the study showed that, the single slice scanner was inferior in terms of noise content, resulting in degraded visualization of small low contrast objects. Image noise characteristics of both multislice scanners appeared comparable and superior to that conventional scanner. Low contrast resolution of 4-multislice CT was comparable or superior to that of the conventional scanner but the low contrast resolution of 64-multislice CT was worse than conventional CT. The single slice and both multislice scanners were superior to conventional CT in terms of both uniformity and high contrast resolution. Slice thickness accuracy in all scanners was comparable. Radiation dose in all scanners trended higher than conventional CT. Slice thickness and pitch were factors affecting image quality and radiation dose for all scanners. Slice thickness was an important factor in controlling image quality and radiation dose in all parameters except $nCTDI_{air}$ of multislice scanners. The changing in pitch impacted on image noise, low contrast resolution, and $CTDI_{vol}$ but did not affect uniformity and high contrast resolution.

Key words *: Computed Tomography ,CT, Physical Performance, Image Quality, CTDI.*

1. Introduction

To increase volume coverage speed, x-ray computed tomography has been developed from axial scan into helical scan[1]. Afterward, several CT manufacturers introduced multiple-row detector CT (MDCT) or multislice CT (MSCT) scanners, multiple detector rows along the z axis are used to simultaneously collect multiple projections[2,3,4]. In helical CT projection acquisition is concurrent with patient translation, whereas in conventional CT these two steps alternate[1].

With the progress of helical scanning, various types of interpolation and reconstruction methods have been proposed such as 360°LI (3600 Linear interpolation), 180°LI, 180°MLI, AMPR (Adaptive Multiple Plane Reconstruction) method[1,4-6]. The development of CT scanner technology has led to difference in slice thickness selection[7]. The impact of kVp, x-ray filtration, tube power and tube cooling limitations, and the relationship between noise and x-ray collimation are fundamentally the same in helical CT as in conventional

CT. On the other hand, helical CT introduces a new factor that also affects the object contrast and slice profile. This new factor is also characterized by the helical pitch[2,8]. On multislice scanners the relationship between pitch and image quality has been studied by several group[6,8-11]. Different of CT scanners and parameters not only affects the range of anatomy that is covered as well as slice thickness, image noise, and contrast resolution, but will also have an impact on how much radiation dose a patient will receive[3,12-21].

2. Material and Methods

This study was performed on to evaluate the effect of different CT scanner types and modes, such as a conventional CT scanner (PQ2000, Picker, Radiology section, Taksin Hospital), a single slice CT system (Asteion, Toshiba, Neuroradiology department, Prasat neurogical institute), two multislice CT scanner (LightSpeed Plus, General Electric Medical Systems, Department of Radiological Technology, Faculty of Medical Technology, Mahidol University and Somatom Sensation 64, Siemens Medical Solutions, Department of Radiology, Queen Sirikit Medical Center, Ramathibodi Hospital).

2.1 Image Quality Determination

Image quality for each scanner were evaluated in terms of image noise, uniformity, low contrast resolution, high contrast resolution and slice thickness accuracy using the commercially available CT performance phantom, Catphan® 600 (The Phantom Laboratory, Department of Radiological Technology, Faculty of Medical Technology, Mahidol University). Methods for determination of these image quality characteristics were based on those described in the Catphan® manual[22]. The scan conditions were selected from head protocols, which mainly derived from those recommended by the manufacture (Table 1).

Image Noise and Uniformity

Image noise and uniformity were evaluated using a uniformity module contained in the Catphan® phantom under the various conditions described above. Noise was expressed as a standard deviation of Hounsfield units for pixels in a circular regions of interest (ROI) approximately 200 mm^2 at the center phantom. CT number uniformity can be assessed by the means CT number were measured in small (approximately 90 mm^2) ROIs at the center and four radial directions near the edges of the phantom. The uniformity was expressed as the largest difference (in Hounsfield units) between a peripheral ROI and the center ROI.

Low Contrast Resolution

Low contrast resolution was determined with the score from visualization and the diameter

Table 1. Scanning parameters.

Scan Mode	Parameters	CT scanners			
		Conventional CT	Single slice CT	4-multislice CT	64-multislice CT
Axial	Tube potential (kV)	120	120	120	120
	Tube current (mA)	150	200	160	380
	Rotation time (s)	2.0	1.0	2.0	1.0
	Filter	smooth	FC29	Standard	H30s
	Slice collimation (mm)	2, 3, 4, 5, 8, 10	1.5, 3, 5, 7, 10	4x 2.50, 4 x 3.75, 4 x 5.00, 2 x 7.50, 2x 10.00	12 x 2.4, 6 x 4.8, 4 x 7.2, 3 x 9.6
Helical	Tube potential (kV)	-	120	120	120
	Tube current (mA)	-	200	300	380
	Rotation time (s)	-	1.0	1.0	1.0
	Filter	-	FL01	Standard	H30s
	Collimator pitch	-	0.5, 1.0, 1.2	0.75, 1.50	0.5, 0.8, 1.2
	Slice collimation (mm)	-	2, 3, 5, 7, 10	4 x 2.50, 4 x 3.75, 4 x 5.00, 2 x 7.50, 2 x 10.00	18 x 1.5, 9 x 3, 6 x 5, 4 x 7 4 x 10

of detectable objects at each contrast level. Low contrast module was used to test low contrast resolution, contained several cylindrical low contrast objects of different sizes arranged in a cycle; the background was of uniform density. To avoid a partial volume effect, the objects 40 mm long in the z axis with various diameters (ie, 2, 3, 4, 5, 6, 7, 8, 9, 15 mm) and deviated from nominal contrast levels by 0.3%, 0.5%, and 1.0% were chosen for the study. The visualization of each object was graded on a three level scale: grade 1.0 was assigned when the object was visible and appeared as a perfect circle, grade 0.5 was assigned when the object was not clearly visible, and grade 0 was assigned when the object could not be detected. The image window width and level were adjusted to provide maximum visibility of all test objects. Window widths and window levels were comparable for each scanner.

High Contrast Resolution

There are two procedures that used to evaluate the high contrast resolution. In the first method used a line pair pattern. After scanning the pattern, the images were visually inspected to determine the smallest resolvable line pair pattern. The second method was calculated based on the modulation transfer function (MTF) by simplified method using technique described by Nickoloff and Riley[23,24]. MTF determined with the used of a tungsten carbide bead (0.28 mm diameter) contained in module CTP528.

Slice Thickness

Slice thickness was determined both counting the beads ramp in the CTP591 module and the average full-width at half maximum (FWHM) of the CT number profile from scanning two pairs of 23° wire ramps contained in the CTP401 module. A trigonometric conversion was calculated by multiplying the wire ramp length with 0.42. To find the FWHM of the wire from the scan image by determination the CT number values for the wire ramp ($CT\#_{ramp}$) and for the background ($CT\#_{bkg}$). Using the CT values, determine the half maximum CT number according to the equation:

$$\text{Half maximum CT \#} = \left(\frac{CT\#_{ramp} - CT\#_{bkg}}{2} \right) + CT\#_{bkg}$$

2.2 Dose Measurement

Exposure dose was measured with the standard measurement method of air CT dose index ($CTDI_{air}$). Results were normalized by tube current exposure time product (mAs) in order to compare scanners. Dose measurements were performed with a 10 cm length pencil ionization chamber (RadCal 10x9-3CT) connected to dosimeter (Radcal 9095, Radcal Corporation, Department of Radiological Technology, Faculty of Medical Technology, Mahidol University). The ionization chamber was placed at the isocenter of the scanner with its axis aligned to the axis of rotation and extended beyond the end of the table in order to exclude attenuation of beam by the table. The exposure (expressed as Roentgens) was obtained with the ionization chamber dosimeter and converted to the values of absorbed dose to air with the f-factor 0.876 cGy/R. To determine the absorbed dose in a scan plane, $CTDI_{air}$ was obtained by the sum of ion chamber output divided by nominal slice thickness. To determine the effects of collimation and pitch on radiation dose, volume ($CTDI_{vol}$) were calculated.

3. Results and Discussion

The resulted of physical performance characteristics were shown in Table 2. The noise was expressed as standard deviation (SD). Figure 1 showed the noise levels of axial scan. The noise levels of single slice scanner were higher than noise levels of conventional scanner for each equivalent slice thickness. For multislice CT scanner, image noise was comparable between 4- and 64-multislice scanners and lower than conventional scanner for each slice thickness. The results showed that noise was dependent on slice thickness and collimator pitch. Decreasing slice thickness or increasing helical pitch the noise

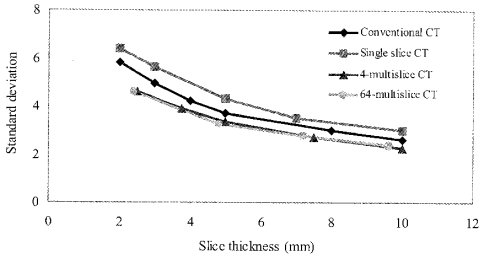

Figure 1. Noise characteristics of axial scan.

levels increase that was reducing the number of transmitted photon in a region of interest and data sampling, lead to larger variations in pixel numbers.

The uniformity data expressed as the maximum difference in CT number between peripheral and center ROI (Table 2). From these uniformity measurements, the conventional scanner showed slightly non-uniformity which average CT number of peripheral ROI were higher than center ROI (5.3-6.4 HU). The single slice and multislice scanner showed the same performance that the values did not differ from the centre by the average CT number less than 1 HU. The images uniformity was no difference as a function of slice thickness or collimator pitch.

Low contrast resolution measurement was evaluated from the minimum diameters of detected cylinders and low contrast score. From the Table 2, performance of the 4-multislice scanner was comparable with conventional scanner and significantly better than that of the single slice and 64-multislice scanner in axial scan. Low contrast detectability depend on slice thickness and pitch when slice thickness was increased or reduced helical pitch the low contrast detectability improved which due to the reduced noise levels. Figure 2, 3 shows images of the low contrast phantom for the 64-multiclice scanner at various slice thickness and helical pitch, respectively. From the Table 2, the detectability of the 1.0% low contrast targets was comparable for each scanner that was detectable at 2-5 mm. For minimum diameter of detected at 0.5% and 0.3% were dependent on helical pitch. The main difference between the performances of the CT appears when trying to detect a contrast level of 0.3%. The same as low contrast scores, conventional and 4-multislice scanner had comparable scores better than of single slice and 64-multislice scanner.

The results of the MTF evaluation were then compared to that obtained from a visual line pair pattern test. A summary of findings were presented in Table 2. The MTF and line pair visualization of conventional CT was poorer in comparison to both single slice and multislice scanner. The results obtained for each scanner were slightly dependent on slice thickness which slice thickness decreased, the MTF improved. The relationship between pitch and high contrast resolution was not as straightforward owing to the variation in z-axis distribution of data samples, created by the interleaving of adjacent multiple helices, at different pitch values. In line pair pattern, when the width and separation of the bars become smaller, the image contrast of the bars will decrease, the visual resolution was decreased.

The results shown in the Table 2 that the FWHM ramp lengths measured for all scanners depend on the slice thickness and scanner type. The width of the radiation beam was consistently within 1 mm of the nominal scan width, exception in single slice CT with slice thickness 10 mm and pitch 1.5 the error was 1.34 mm with the ramp-determined. In conventional and single slice scanner, the data suggest that the difference between actual and nominal slice thickness were quite large for small collimations but the error of multislice scanners were increased as the slice thickness increased. In conventional and single slice scanners, slice thickness was determined mainly by collimator, while multislice CT was defined by the width of the detectors in the slice

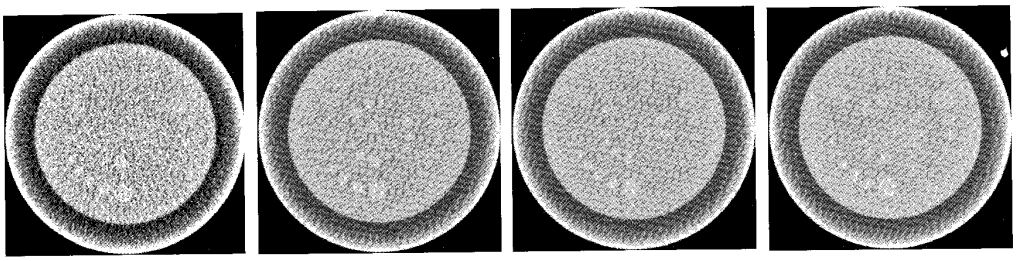

(a) (b) (c) (d)

Figure 2. Low contrast phantom images of 64-multislice scanner with various slice thickness. (a) 2.4 mm, low contrast score 7.5, (b) 4.8 mm, low contrast score 8.0, (c) 7.2 mm, low contrast score 9.5, (d) 9.6 mm, low contrast score 9.5

Table 2. Scanning parameters and results.

Scanners	Scan mode	Slice thickness (mm)	Noise	Uniformity	Low contrast resolution				High contrast resolution		Slice thickness accuracy
			Standard deviation (SD)	Maximum difference in CT number (HU)	Minimum diameter detectable (mm) 1%	0.5%	0.3%	Scores	5%MTF (lp/cm)	Visualization (lp/cm)	Difference from nominal slice thickness (mm)
Conventional CT	Axial scan	2	5.84	6.4	2	4	-	14.0	6.09	7	0.31
		3	4.97	6.4	2	3	-	14.5	6.03	7	0.36
		4	4.23	5.3	2	3	15	15.5	5.84	7	0.20
		5	3.71	5.4	2	3	9	16.0	5.65	7	0.04
		8	3.01	5.4	2	3	7	18.0	5.30	6	-0.13
		10	2.65	5.3	2	3	7	18.0	5.25	6	-0.03
Single slice CT	Axial scan	2	6.41	0.52	3	8	-	9.0	6.80	8	0.21
		3	5.63	0.59	2	6	-	11.0	6.66	8	0.15
		5	4.34	0.37	2	5	15	12.5	6.55	8	-0.07
		7	3.53	0.21	2	4	9	14.0	6.48	8	-0.07
		10	3.01	0.19	2	4	8	14.5	5.83	7	-0.03
	Helical scan/ pitch 0.5	2	6.10	0.40	3	4	-	12.5	6.13	7	0.52
		3	5.05	0.44	2	4	15	15.0	6.11	7	0.36
		5	4.02	0.13	2	4	7	17.0	5.86	7	0.25
		7	3.21	0.35	2	3	6	18.5	5.65	6	0.35
		10	2.67	0.29	2	3	5	19.5	5.16	6	0.40
	Helical scan/ pitch 1.0	2	6.42	0.41	4	8	-	8.0	6.81	8	0.52
		3	5.40	0.44	3	6	-	10.0	6.81	8	0.36
		5	4.25	0.26	3	6	15	10.5	6.13	7	0.46
		7	3.52	0.18	3	5	15	11.5	6.10	6	0.67
		10	2.89	0.12	3	5	9	12.5	5.60	6	0.92
	Helical scan/ pitch 1.2	2	6.72	0.47	4	9	-	7.5	6.14	7	0.52
		3	5.83	0.34	4	7	-	8.5	5.95	7	0.68
		5	4.56	0.22	4	6	15	9.5	5.70	7	0.77
		7	3.71	0.02	4	6	15	9.5	5.67	6	0.98
		10	3.19	0.13	3	6	15	10.5	5.62	6	1.34
4-multislice CT	Axial scan	2.50	4.61	0.53	2	4	9	14.5	8.79	10	0.02
		3.75	3.93	0.43	2	4	7	16.5	8.67	10	0.03
		5.00	3.35	0.32	2	3	7	17.5	7.76	9	0.04
		7.50	2.72	0.46	2	3	6	18.0	7.43	8	0.06
		10.00	2.29	0.39	2	3	5	18.5	7.28	8	0.08
	Helical scan/ pitch 0.75	2.50	4.40	0.31	3	4	8	15.0	7.88	9	0.02
		3.75	3.77	0.20	3	3	6	17.0	7.81	9	0.03
		5.00	3.16	0.10	3	3	5	17.5	7.62	9	0.04
		7.50	2.26	0.25	3	3	5	18.5	7.15	8	0.17
		10.00	1.99	0.37	3	3	5	18.5	6.33	7	0.19
	Helical scan/ pitch 1.50	2.50	6.04	0.51	4	7	-	8.0	8.79	9	0.02
		3.75	4.61	0.38	4	6	15	9.5	7.99	9	0.03
		5.00	4.03	0.57	4	6	15	9.5	7.53	8	0.04
		7.50	3.12	0.49	4	6	15	9.5	6.49	7	0.17
		10.00	2.74	0.39	4	5	9	11.0	6.03	7	0.29
64-multislice CT	Axial scan	2.4	4.6	0.7	3	15	-	7.5	7.90	9	-0.03
		4.8	3.3	0.1	3	9	-	8.0	7.59	9	0.03
		7.2	2.8	0.3	3	7	-	9.5	7.39	8	0.13
		9.6	2.4	0.3	3	7	-	9.5	7.29	8	0.26
	Helical scan/ pitch 0.5	1.5	5.2	0.8	3	-	-	7.0	6.41	7	-0.02
		3.0	3.9	0.5	3	9	-	8.5	6.08	7	0.00
		5.0	2.9	0.2	3	6	-	10.5	6.02	7	0.09
		7.0	2.5	0.6	3	6	-	10.5	5.45	6	0.17
		10.0	2.2	0.5	3	5	-	11.5	5.42	6	0.37
	Helical scan/ pitch 0.8	1.5	5.5	0.4	4	-	-	6.0	6.66	8	-0.01
		3.0	4.3	0.4	3	15	-	7.5	6.64	8	0.01
		5.0	3.5	0.2	3	9	-	8.0	6.57	8	0.09
		7.0	2.8	0.3	3	8	-	9.0	6.46	7	0.20
		10.0	2.7	0.6	3	8	-	9.0	5.73	7	0.41
	Helical scan/ pitch 1.2	1.5	7.0	0.3	5	-	-	4.5	6.70	8	0.00
		3.0	4.9	0.4	4	15	-	6.0	6.70	8	0.03
		5.0	3.7	0.8	4	15	-	6.0	6.55	8	0.10
		7.0	3.2	0.5	4	15	-	6.0	6.40	7	0.21
		10.0	2.9	0.3	4	15	-	6.0	5.89	7	0.45

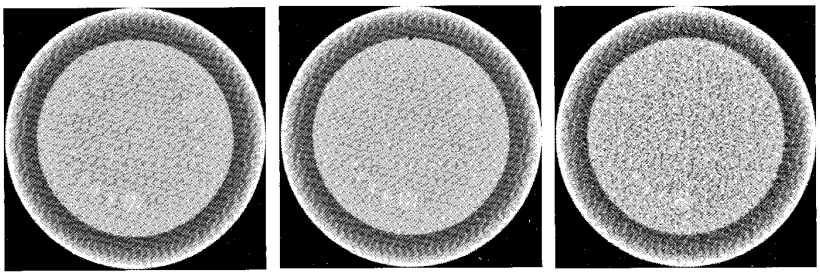

(a) (b) (c)

Figure 3. Low contrast phantom images of 64-multislice CT at slice thickness 5.0 mm with various collimator pitch. (a) pitch 0.5, low contrast score 10.5, (b) pitch 0.8, low contrast score 8.0, (c) pitch 1.2, low contrast score 6.0.

thickness dimension. The width of the detector was changed by binding different numbers of individual detector elements together. The error of slice thickness was dependent on the number of detector elements which increased as the numbers of detector elements increased. In case of helical mode scanning yields poorer slice thickness accuracy, as compared to axial mode scanning. This can be attributed to the table motion and subsequent interpolation process characteristic of helical scan.

The results of the pencil ion chamber measurements for each examination were shown in Table 3, 4. CTDI values on the single slice and 4-multislice scanners were higher than those of conventional scanner but radiation dose in 64-multislice CT was lower than conventional CT. For conventional and single slice scanner, slice thickness had a relationship to dose. The CTDI normalized increased for smaller collimation widths which may be larger penumbra. In multislice CT, slice thickness was not a factor to investigate radiation dose characteristics. Instead, total nominal scan width was the factor affecting the dose. That dose values decreased when the total nominal scan width increased. The penumbral effect in multislice CT could be minimized by imaging with radiation beam with the widest available nominal x-ray beam width. For helical scan the average dose was influenced by the pitch factor. For example, the actual dose decreased when the pitch factor was larger than 1, and increased when the pitch factor was smaller than 1 (for constant mA) Radiation dose estimates for helical scan were expressed as $CTDI_{vol}$ (in Gy).

4. Conclusion

Slice thickness and pitch were factors affecting image quality and dose of 4 scanners. From this study found that slice thickness was important factor controlling image quality and radiation dose in all scanners except $nCTDI_{air}$ in multislice system. The thicker slice was better image noise and low contrast resolution but decreasing high contrast resolution. The impact of changing in pitch was impact in image noise, low contrast resolution, and $CTDI_{vol}$ in all scanners by decreasing helical pitch reduced image noise, better low contrast resolution but increasing in $CTDI_{vol}$.

The conventional scanner was worse than single slice and multislice scanners in term of uniformity and high contrast resolution. The noise level of conventional scanner was lower than single slice scanner for each equivalent slice thickness but higher than multislice scanners both 4- and 64-multislice CT. Low contrast resolution of conventional scanner was comparable with 4-multislice CT and significantly better than single slice and 64-multislice scanner. The impact of slice thickness and pitch were most apparent in detectability of low contrast level of 0.3% and not significantly different on low contrast level of 1.0%. Slice thickness accuracy was approximate ±1 mm in all scanners. The slice thickness accuracy in helical scan was slightly poorer than axial scan.

Radiation dose of conventional CT was lower than single slice and 4-multislice scanners but higher than 64-multislice CT. In single slice

Table 3. Radiation dose characteristics in axial mode.

Scanners	Slice thickness (mm)	$CTDI_{air}$ (mGy)	$nCTDI_{air}$ (mGy/100mAs)
Conventional CT	2.00	64.50	21.50
	3.00	64.60	21.53
	4.00	64.28	21.43
	5.00	63.88	21.29
	8.00	63.82	21.27
	10.00	63.44	21.15
Single slice CT	2.00	121.97	40.66
	3.00	100.74	33.58
	5.00	94.42	31.47
	7.00	93.81	31.27
	10.00	93.82	31.27
4-multislice CT	2.50	101.70	31.78
	3.75	100.78	31.49
	5.00	92.46	28.89
	7.50	100.62	31.44
	10.00	92.43	28.89
64-multislice CT	2.40	62.52	16.45
	4.80	62.54	16.46
	7.20	62.57	16.47
	9.60	62.58	16.47

Table 4. Radiation dose characteristics in helical mode compare with axial scan.

Scanners	Scan mode	$CTDI_{vol}$ (mGy)
Single slice CT	Axial scan	101.0
	Helical scan/ pitch 0.5	201.9
	Helical scan/ pitch 1.0	101.0
	Helical scan/ pitch 1.2	84.1
4-multislice CT	Axial scan	97.6
	Helical scan/ pitch 0.75	122.0
	Helical scan/ pitch 1.50	61.0
64-multislice CT	Axial scan	62.6
	Helical scan/ pitch 0.5	125.1
	Helical scan/ pitch 0.8	78.2
	Helical scan/ pitch 1.2	52.1

system, slice thickness was impact on $nCTDI_{air}$. In multislice system, slice thickness was not impact on $nCTDI_{air}$ but affecting by beam collimation or detector configuration. For helical scan, $CTDI_{vol}$ was inversely proportional to pitch in all scanners.

5. Acknowlagement

This work was supported in part by the Department of Radiology, Faculty of Medical Technology, Mahidol University, Assist. Prof. Sawwanee Asavaphatiboon (Department of Radiology, Sirikit Medical Center, Ramathibodi Hospital), Archan Nuttawan Jangsri (Radiology section, Taksin Hospital), and Ms. Kamolwan Srisubut (Department of Neuroradilogy, Prasat Neurogical Institute) for their helpful support on using of the CT scanners.

Reference

1. Crawford CR, King KF. Computed tomography scanning with simultaneous patient translation. Med Phys 1990;17(6):967-82.
2. Fuchs T, Kachelrieß M, Kalender WA. Technical advances in multi-slice spiral CT. Eur J Radiol 2000;36(2):69-73.
3. Kulama E. Scanning protocols for multislice CT scanners. Br J Radiol 2004; 77: 2-9.
4. 4.Flohr TG, Schaller S, Stierstorfer K, Bruder H, Ohnesorge BM, Schoepf, UJ. Multi-detector row CT systems and image-reconstruction techniques. Radiology 2005;235:756-73.
5. Taguchi K, Aradate H. Algorithm for image reconstruction in multi-slice helical CT. Med Phys 1998;25(4):550-61.

6. Flohr TG, Stierstorfer K, Ulzheimer S, Brudre H, Primak AN, McCollough CH. Image reconstruction and image quality evaluation for a 64-slice CT scanner with z-flying focal spot. Med Phys 2005;32(8):2536-47.
7. Hsieh J. Investigation of the slice sensitivity profile for step-and-shoot mode multi-slice computed tomography. Med Phys 2001;28(4): 491-500.
8. McCollough CH, Zink FE. Performance evaluation of a multi-slice CT system. Med Phys 1999;26(11):2223-30.
9. Hu H, Fox SH. The effect of helical pitch and beam collimation on the lesion contrast and slice profile in helical CT imaging. Med Phys 1996;23(12):1943-54.
10. Wang G, Vannier MW. The effect of pitch in multislice spiral/helical CT. Med Phys 1999; 26(12):2648-53.
11. Hu H, He HD, Foley WD, Fox SH. Four Multidetector-row helical CT: Image quality and volume coverage speed. Radiology. 2000;215: 55-62.
12. Southon FC. CT scanner comparison. Med Phys 1981;8(1)(Technical notes):62-75
13. Seifert H, Hagen T, Bartella K, Blass G, Piepgras U. Patient doses from standard and spiral CT of the head using a fast twin-beam system. Br J Radiol 1997;70(839):1139-45.
14. Scheck RJ, Coppenrath EM, Kellner MW, Lehmann KJ, Rock C, Rieger J, Rothmeier L, Schweden F, Bauml AA, Hahn k. Radiation dose and image quality in spiral computed tomography: multicentre evaluation at six institutions. Br J Radiol 1998;71(847):734-44.
15. Smith A, Shah GA, Kron T. Variation of patient dose in head CT. Br J Radiol 1998;71: 1296-301.
16. McNitt-Gray MF, Cagnon CH, Solberg TD, Chetty I. Radiation dose in Spiral CT: the relative effects of collimation and pitch. Med Phys 1999;26(3):409-14.
17. Nicholson R, Fetherston S. Primary radiation outside the imaged volume of a multislice helical scan. Br J Radiol 2002;75:518-22.
18. McNitt-Gray MF. AAPM/RSNA Physics tutorial for residents: topics in CT. Radiographics 2002;22:1541-53.
19. Thornton FJ, Paulson EK, Yoshizumi TT, Frush DP, Nelson RC. Single versus multidetector row CT: Comparison of radiation doses and dose profiles. Acad Radiol 2003; 10:379-85.
20. Nickoloff EL, Dutta AK, Lu ZF. Influence of phantom diameter, kVp and scan mode upon computed tomography dose index. Med Phys 2003;30(3):395-402.
21. Mori S, Endo M, Nishizawa K, Murase K, Fujiwara H, Tanada S. Comparison of patient doses in 256-slice CT and 16-slice CT scanners. Br J Radiol 2006;79:56-61.
22. The phantom laboratory. Catphan® manual. Available from: URL: http://www.phantomlab.com/
23. Nickoloff EL, Riley R. A simplified approach for modulation transfer function determinations in computed tomography. Med Phys 1985;12 (4):437-42.
24. Mongkolsuk M, Thumwerapong W, Jangsri N. An evaluation of spatial resolution in computed tomography. Thai J Radiological Tech 2001; 26(2): 13-20.